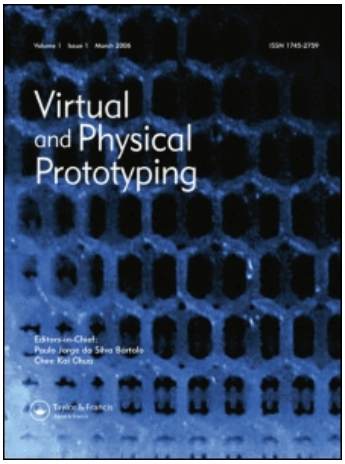

Virtual and Physical Prototyping
Publication details, including instructions for authors and subscription information:
http://www.informaworld.com/smpp/title~content=t716100703

Virtual and physical prototyping by means of a 3D optical digitizer: Application to facial prosthetic reconstruction

Giovanna Sansoni[a]; Gianluca Cavagnini[a]; Franco Docchio[a]; Giorgio Gastaldi[b]
[a] Department of Electronics for the Automation, University of Brescia, Brescia, Italy [b] Removable Prosthodontics School of Dentistry, Piazzale Spedali Civili, University of Brescia, Brescia, Italy

Online publication date: 03 December 2009

To cite this Article Sansoni, Giovanna , Cavagnini, Gianluca , Docchio, Franco and Gastaldi, Giorgio(2009) 'Virtual and physical prototyping by means of a 3D optical digitizer: Application to facial prosthetic reconstruction', Virtual and Physical Prototyping, 4: 4, 217 — 226
To link to this Article: DOI: 10.1080/17452750903236658
URL: http://dx.doi.org/10.1080/17452750903236658

Virtual and Physical Prototyping, Vol. 4, No. 4, December 2009, 217–226

Taylor & Francis
Taylor & Francis Group

Virtual and physical prototyping by means of a 3D optical digitizer: Application to facial prosthetic reconstruction

Giovanna Sansoni[a]*, Gianluca Cavagnini[a], Franco Docchio[a] and Giorgio Gastaldi[b]

[a]Department of Electronics for the Automation, University of Brescia, via Branze 38, Brescia, I-25123 Italy
[b]Removable Prosthodontics School of Dentistry, Piazzale Spedali Civili, University of Brescia, Brescia, I-25123 Italy

(*Received 25 March 2009; final version received 23 June 2009*)

In this article, optical 3D acquisition, reverse engineering and rapid prototyping are proposed for virtual sculpturing and fabrication of facial prostheses. A novel approach to the direct mould production by means of rapid prototyping fabrication is introduced. Full coverage of the surface is obtained by using multi-view acquisition and alignment of point clouds. Suitable topological description is provided by triangle tessellation. Depending on the clinical case, one or two prototypes can be used either to directly cast the final prosthesis or to fabricate the positive wax pattern. The method has been applied to the development of a nose prosthesis; its generality is investigated in the case of virtual ear modelling. The advantages with respect to known art manufacturing methods are addressed.

Keywords: 3D imaging sensors; reverse engineering; rapid prototyping; maxillofacial prosthetic reconstruction

1. Introduction

In the last decades, the use of three-dimensional instrumentation for the contact-less gauging of surfaces has become increasingly relevant in many fields. An impressive number of techniques and systems have been developed for the fast acquisition and the reverse engineering of complex shapes: the goal is to capture in short times and at reasonable accuracies (and costs) free-form shapes, in view of their reshaping and prototyping (Blais 2004). The concepts and the methodologies underlying these processes have found fruitful exploitation in many applications, spanning from the traditional quality control in the industrial and manufacturing production, to the restitution of heritage, to the virtual reality world, and to medicine applications (Sansoni *et al.* 2009).

An interesting field of application is represented by the development of prostheses in post-oncological reconstruction and in congenital defect treatment of the human face. Both the functional and the aesthetic characteristics of the prosthesis are crucial, in view of allowing the patients to overcome either the social, the psychological and the economic problems deriving from their handicap (Brasier 1954, Roberts 1971). Traditional reconstruction techniques are based on (i) impression making procedures, to obtain the negative patterns of the site of the deformity, (ii) plaster casting of negative patterns, to retrieve the positive defects, (iii) construction of wax positive replicas of the actual prosthesis, (iv) conventional flasking and investing procedures, to obtain the negative mould, and (v) casting of suitable materials into the negative mould, to obtain the definitive, actual prosthesis (Taylor 2000). These procedures present a number of inadequacies. Firstly, impression making may cause patient discomfort and stress. In addition, the pressure that must be applied on the face to guarantee the required quality of the impression, inherently deforms soft tissues, and precludes accurate duplication of

*Corresponding author. Email: giovanna.sansoni@ing.unibs.it

Virtual and Physical Prototyping
ISSN 1745-2759 print/ISSN 1745-2767 online
http://www.tandf.co.uk/journals
DOI: 10.1080/17452750903236658

the anatomy of the face. Secondly, the quality of the wax positive replica is dependent on the artistic skills of an experienced prosthetist. The performance of the process depends on both shape and extension of the defect, as well as on the possibility of exploiting the face symmetry to grasp the shape of the lost part, as in the case of eye or ear reconstruction. Hence, human error contribution, subjectivity in the reconstruction, low reproducibility of the process, and poor initial shape information often lead to serious misfitting of the final prosthesis, under both functional and aesthetical viewpoints. Finally, the overall process is not adaptive, i.e., whenever the existing prosthesis should be replaced, the overall process must be performed again.

The purpose of this research activity is to develop a novel approach that combines optical three-dimensional acquisition, reverse engineering (RE) and rapid prototyping (RP) for mould production in the prosthetic reconstruction of facial prostheses. The manufacturing system proposed in this work does not require initial casts and, in principle, it uses RP to fabricate the physical mould without the need of positive patterns. Hence, the dependence on the anaplasthologist skill is significantly reduced, and the overall process efficiency is increased. The proposed method is general and can be applied to clinical cases where the missing anatomic part is unique, as in the case of a nose, as well as to cases where the contralateral organ is available, as in the case of an ear.

This paper is structured as follows. In Section 2, the overview of the methodology is described. In Section 3 two experimental cases are discussed. The former is the fabrication of a nose prosthesis; the latter is the ear virtual modeling. Section 4 presents a discussion and the conclusions.

2. Overview of the method

The method is based on the sequence of six tasks. These are (i) optical acquisition, (ii) multi-view alignment, (iii) polygon model generation, (iv) STL file generation, (v) RP machining of the part and (vi) fabrication of the prosthetic element, presented as follows:

2.1 *Task 1: optical acquisition*

This task is aimed at optically acquiring the target surfaces. The Konica Minolta Vivid 910 laser stripe scanner is used. It is portable, easily configurable, fast, accurate and able to perform the measurements over an extended range. The system can be mounted on a tripod and properly oriented into the measurement volume to optimize the acquisition viewpoint. It is equipped with three lenses, denoted as WIDE (8 mm focal length), MIDDLE (14 mm focal length) and TELE (25 mm focal length). The whole area can be captured in 2.5 seconds (FINE mode) or in 0.3 seconds (FAST mode). Typical values of the measurement parameters are listed in Table 1 (Konica Minolta Sensing, Inc. 2002). The software package embedded in the instrument produces 3D point clouds that can be easily exported into very powerful elaboration environments, for the virtual prototyping of the models and for their rapid prototyping by means of RP machines.

Table 1. Measurement specifications of the Konica Minolta Vivid 910 optical digitiser.

	Wide lens	Middle lens	Tele lens
Focal distance	8 mm	14 mm	25 mm
Object distance range	0.6 to 2 m	0.6 to 2.5 m	0.6 to 2.5 m
Field of view	0.6 to 1.2 m	0.6 to 1.2 m	0.6 to 1.2 m
X range	359 to 1196 mm	198 to 823 mm	111 to 463 mm
Y range	269 to 897 mm	148 to 618 mm	83 to 347 mm
Z range	110 to 750 mm	70 to 800 mm	40 to 500 mm
X accuracy	$\pm$1.40 mm	$\pm$0.38 mm	$\pm$0.22 mm
Y accuracy	$\pm$1.04 mm	$\pm$0.31 mm	$\pm$0.16 mm
Z accuracy	$\pm$0.40 mm	$\pm$0.20 mm	$\pm$0.10 mm

2.2 *Task 2: multi-view alignment*

Task 2 is aimed at registering the set of acquired point clouds into a common reference frame. A first requirement is to keep under control the errors that sum up during the alignment. The alignment software should provide suitable parameters to quantitatively evaluate the alignment performance, and to avoid unpredictable error propagation. Among the software tools available, we chose the *IMAlign* module to perform the view alignment (PolyWorks InnovMetric Inc., Canada). It performs pair-wise alignments based on the iterative closest point (ICP) algorithm, and by means of a semi-automatic procedure. After that, the whole alignment is carried out in a completely automatic way. *IMAlign* guarantees high reliability and computational efficiency, provides error histograms and maps for measuring the quality of the alignment, performs multi-view fusion and minimises the measurement noise for improved quality of the triangle mesh (Chen *et al.* 1992).

An additional requirement for optimal alignment accuracy is to keep the number of views at a minimum, without sacrificing the measurement resolution. The achievement of this compromise can be obtained by a measurement strategy that is based on the build-up of a low/medium-resolution shell of the overall surface, followed by the acquisition of a higher number of high-resolution views. These views are aligned using the shell as the 'skeleton' (Guidi *et al.* 2003). The skeleton is then discarded. The Vivid 910 system proves to be particularly suitable to implement this strategy, since it can provide a variable

measurement resolution without requiring time-consuming calibration. Finally, the aligned views are fused in a single point cloud: even this step is accomplished by the *IMAlign* module.

2.3 *Task 3: generation of the triangle model*

In this task, the point cloud is transformed into models based on the topological connection of simple geometrical elements, which tessellate the shapes. The PolyWorks *IMMerge* module is used. It allows the operator to finely adjust the value of a number of parameters that make this step as flexible as possible, and optimises the mesh both in terms of accuracy with respect to the original point cloud and in terms of number of model triangles (Bernardini and Rushmeier 2002).

2.4 *Task 4: generation of the STL file*

In this task, the triangle mesh is edited and topologically controlled, with a view to producing the STL closed file, to be used by a stereo-lithography machine. The PolyWorks *IMEdit* module carries out this task. It is a very powerful tool for mesh editing, by means of quasi-automatic transformations (for example, 'fill hole' operations, surface smoothing, triangle optimisation). In addition it is equipped with specific functions to reliably reconstruct even seriously corrupted portions of the surface. Following optimisation, the mesh is generally compressed. The PolyWorks *IMCompress* module is used to obtain meshes from the original model, characterised by lower file dimensions. It is thus possible to choose the optimal trade-off between accuracy of the representation and memory use among the sets of meshes.

2.5 *Task 5: RP fabrication*

RP fabrication comprises a wide typology of specific techniques that build a part layer by layer (Chua *et al.* 2000). Among these, SLA is a process that combines CAD/mesh modelling, chemistry and optical laser scanning technologies to produce solid 3D models. Input STL models are horizontally sectioned into thin cross-sections. Inside the stereolithography chamber of the apparatus, an ultraviolet laser traces the first layer of the part on a metal platen, submerged just below the surface of a vat of photosensitive polymer. Wherever the laser interacts with the liquid, this is polymerised and solidifies. Once the layer is traced, the platen sinks the thickness of a layer below the level of the liquid. A sweeper bar moves across the surface of the last layer, making sure there is the exact amount of resin on top. The next layer is then built upon the previous layer. In this manner the entire part is built from the bottom up to the top, with the completed sections of the part remaining submerged.

2.6 *Task 6: fabrication of the prosthesis*

The final task is the fabrication of the prosthesis. The proposed method allows either the production of positive wax patterns or the direct fabrication of the actual prosthesis, depending on the prosthetic material. In the former case, hot cured materials and conventional flasking and investing procedures are required. In the latter case, cold cured materials are directly cast into negative moulds.

3. Experimental cases

3.1 *Making a nose prosthesis*

In this case study, the patient suffered from a total loss of the nose, because of excision of a tumour. Typology and dimension of the facial defect suggested the capture of the whole face, since the deformity was large and central with respect to the face. In addition it was necessary to acquire the lost part from healthy donors. The general method described in Section 1 was applied following the flow-chart shown in Figure 1.

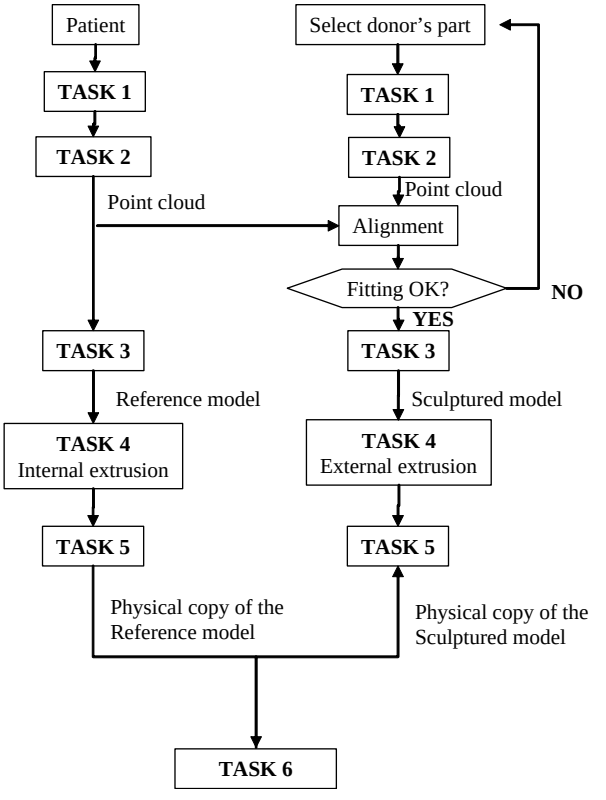

Figure 1. Flow-chart of the process followed to fabricate the nose prosthesis.

In Task 1, the system was mounted on a tripod and properly oriented to optimise the acquisition view point. The patient was comfortably sitting on the dentistry chair. The WIDE lens was used to gauge the whole face, and the FAST acquisition mode was selected. The corresponding point cloud showed a measurement resolution equal to 320 μm. Then, the TELE lens was mounted, and five partial views were captured in the FINE mode scanning. In this case, the measurement resolution was 170 μm. The sensor was then used to gauge at the best resolution (TELE lens, FINE mode) the point cloud of the nose from a suitable number of donors. It was necessary to perform multi-view acquisition following the same procedure as that implemented for the face, due to the high variability of the shapes and to the presence of undercuts and shadow regions.

In Task 2, the alignment of the views was carried out for both the face and the noses, following the procedure described in Section 1.2.1. The higher-resolution, partial views were aligned together using the one acquired at the lowest resolution as the skeleton. The skeleton was then discarded. In this way, it was possible (i) to control the influence of the alignment errors, (ii) to reduce holes and (iii) to guarantee the complete coverage of the surfaces.

Figure 2 shows the result of the alignment for both the face and two noses. The maximum alignment error was 0.4 mm for the face and 0.7 mm for the noses. This was due to the influence of the donor movement and to the limited overlapping among the small nose views.

At this step of the process, the point cloud of each candidate nose was positioned on the point cloud of the face. The possibility of visualising the result in the 3D environment allowed both the operator and the patient to preview the final appearance of the face, to select the point cloud which yielded the most aesthetic improvement, and to add modifications to optimise the shape, the position and the functional fitting of the prosthesis. Eventually, the selected nose was aligned to the face as in Figure 2a.

In Task 3, the aligned point clouds of both the original face and the 'repaired' face were fused, and input to the *IMMerge* module, which generated the two triangle meshes that are referred to as 'Reference model' and 'Sculptured model' in Figure 1. The main requirement was to obtain a reliable adherence to the details of the original face, especially in the proximity of the deformity, and to refine and finely blend the nose to the deformity site, to optimize the functionality and the proportions of the prosthesis in the Sculptured model. In order to maintain the highest fidelity of each model to the original surfaces, a very dense tessellation was chosen, as is evident in the wireframe representation of the models in Figure 3.

In Task 4, very little editing was performed, due to the high quality of the meshes, and to the need to leave the surfaces as close as possible to the original shapes. The *IMEdit* module was used to add a 4 mm internal thickness to the Reference model, and a 4 mm external thickness to the Sculptured model. After that, the meshes were topologically controlled to guarantee the consistency of the triangles, and were saved in two STL files, for their subsequent prototyping. Figure 4 shows the models after the extrusion. The original face, with the defect in correspondence with the sculptured nose, is well visible. Figure 5 plots the intersection of the two meshes with the sagittal plane: they perfectly match in correspondence with the face regions that are not affected by the deformity. On the other hand, in correspondence with the deformity, their shape delimits the volume that should be cast by the material used to fabricate the actual prosthesis. This space is the mould.

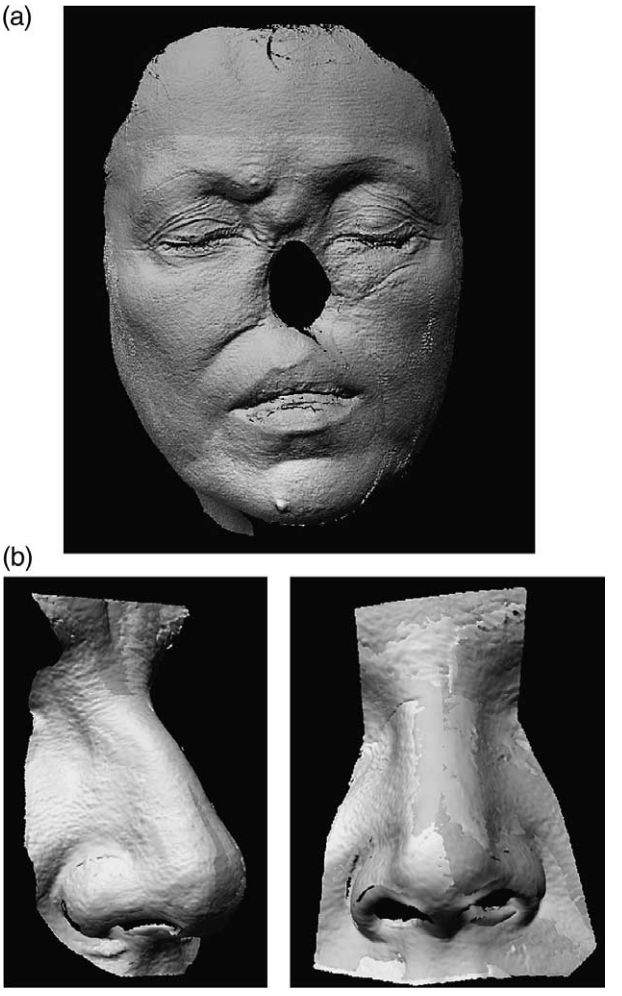

Figure 2. Performance of Task 2. (a) Aligned point clouds of the patient's face; (b) aligned point clouds of two donor noses.

In Task 5, the physical copies were created. Both STL files were sent through the internet for RP machining. They were fabricated using the epoxy photo-polymerizing resin'-Somos Watershed 11120' by the SLA 3500 Prototyping

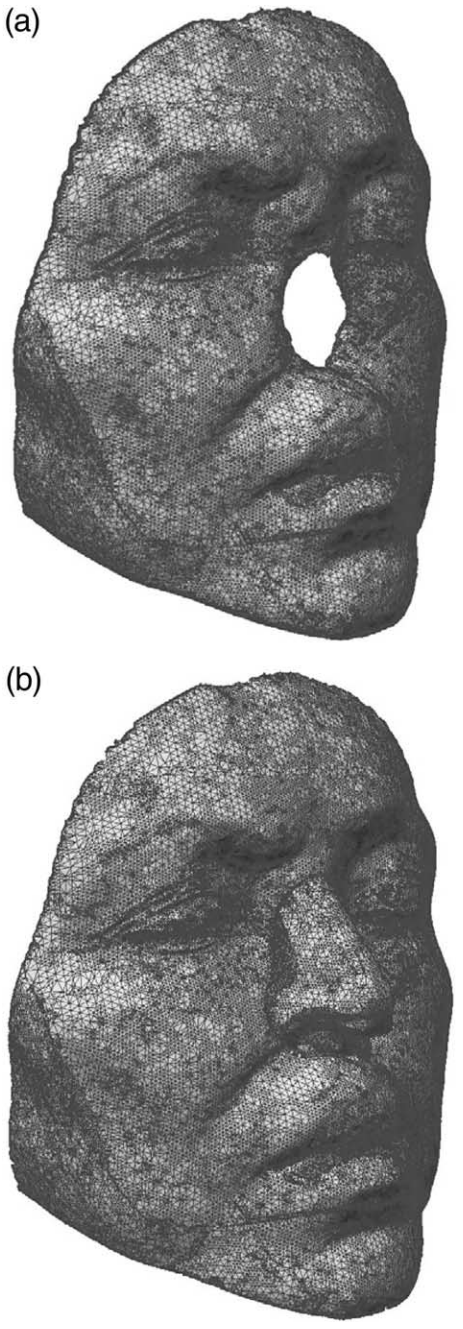

Figure 3. Creation of the meshes. (a) Reference model; (b) Sculptured model.

Machine. The apparatus is characterised by quite satisfactory tolerances ($\pm$0.005" for the initial inch, plus an additional 0.0015" for each additional inch), and by reasonable production times. The two physical models are shown in Figure 6.

In Task 6, the prosthetic element was fabricated. Since hot-cured materials provide the best aesthetic and mechanical performances, the wax positive pattern was cast in this

Figure 4. Virtual superposition of the Sculptured model (9.4 MB STL file) onto the Reference model (11.3 MB STLfile).

experiment. To perform this task, the two physical models were physically overlapped with each other and the wax was poured as shown in Figure 7. The wax pattern was then extracted from the mould and positioned on the prototype of the Reference model as shown in Figure 8. In this way, it was possible to perform the try-in of the prosthesis and its refinement on this copy, without disturbing the patient. The definitive prosthesis was obtained by conventional flasking and investing procedures (Beumer *et al.* 1996). Figure 9 shows the patient's aspect after the positioning of the prosthesis. It was then manually refined on the patient's face, to match the skin colour and texture.

3.2 *Making an ear prosthesis*

In this case study, the general method described in Section 1 was implemented following the flow chart shown in Figure 10. The patient suffered the excision of the left ear.

Fifteen views of the face were acquired and aligned (Task 1 and Task 2). All these views were necessary because of the presence of undercuts and shadows, especially in correspondence with the right ear. In fact this was a serious

Figure 5. Section of the two models along the sagittal plane.

problem, but, after a careful preliminary analysis, the acquisition of the patient's face and of the contralateral organ were satisfactorily performed. Figure 11 shows the

Figure 6. Physical copies obtained by means of SLA machining.

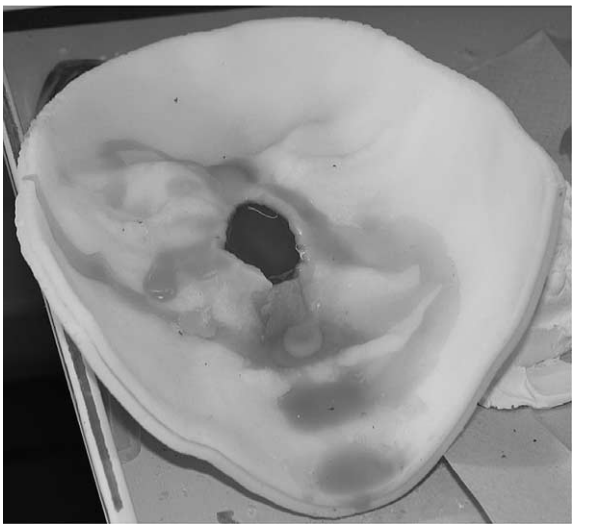

Figure 7. Fabrication of the nose wax positive pattern.

quality of the measurement in correspondence to the ear. After that, the ear was mirrored with respect to the sagittal plane of the face. The resulting point cloud was then carefully aligned to the face, and positioned in

Figure 8. Try-in of the wax nose pattern onto the physical copy of the Reference model.

Figure 9. Prosthesis of the nose.

correspondence with the defect on the left. The Sculptured model was then created (Task 3). It is shown in Figure 12.

The availability of this model was strategic in view of optimising the quality of the prosthetic element prior to its fabrication: the *IMEdit* module allowed us to inspect the model by using metric grids, as shown in Figure 13a; in addition it was possible to define a suitable number of planes that were of great help in obtaining the correct alignment of the prosthetic element with respect to the right ear (Figure 13b).

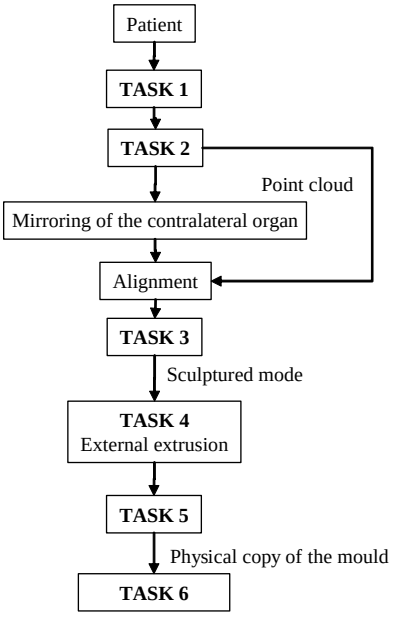

Figure 10. Flow-chart of the process for fabricating the ear prosthesis.

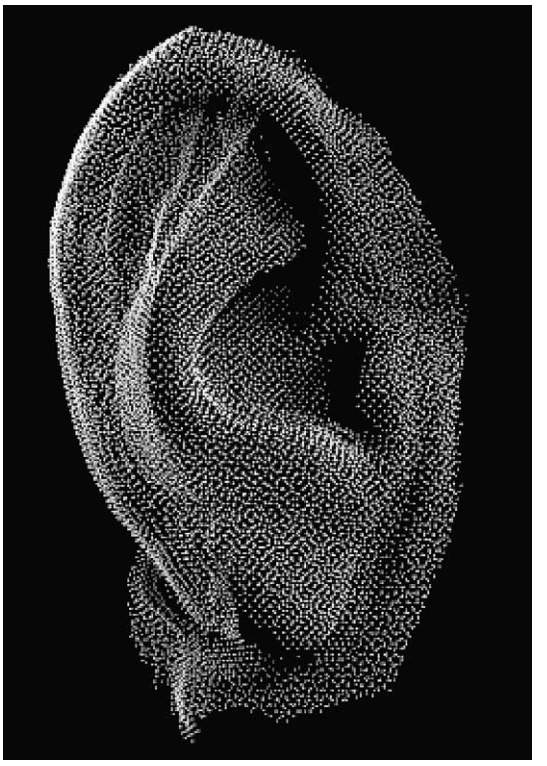

Figure 11. Point cloud of the right ear.

After this step, the region to be reconstructed was selected and externally extruded (Task 4). The result is shown in Figure 14: the virtual sculpturing process naturally blends the shapes of the face in correspondence with the boundaries of the defect. This model in fact represents the virtual mould of the left ear, and, in principle, it is

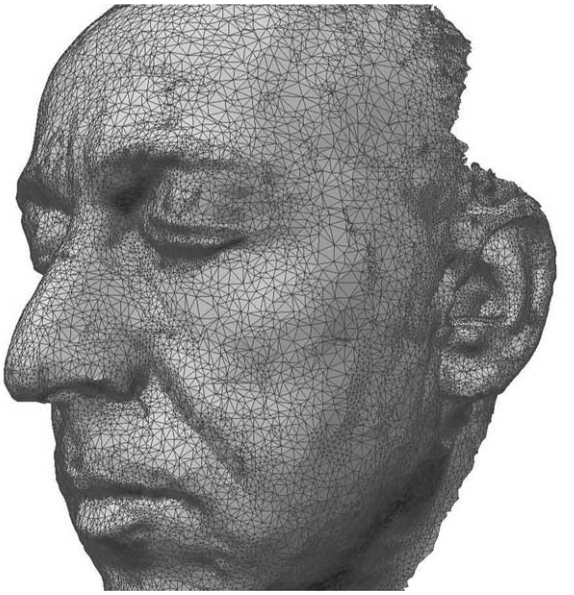

Figure 12. Sculptured model.

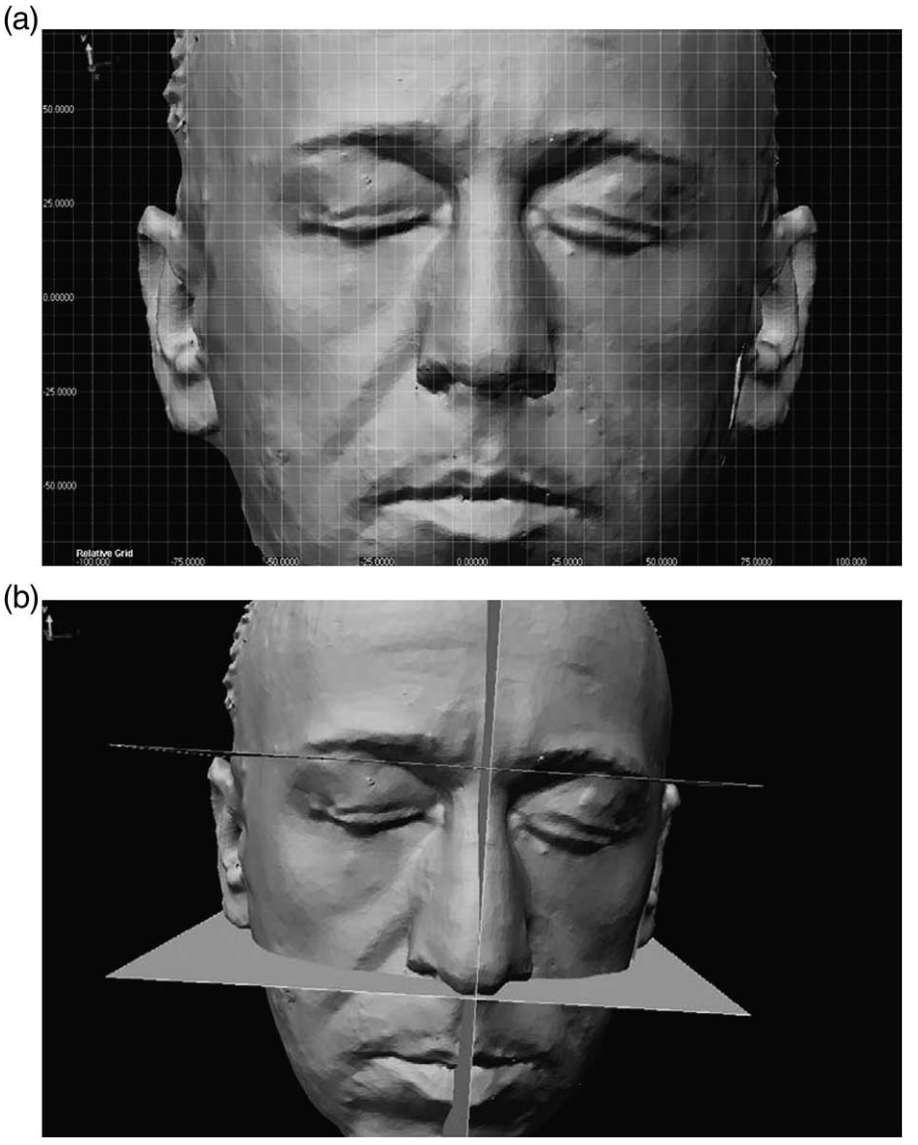

Figure 13. Virtual positioning of the left ear: (a) use of metric grids; (b) intersection with reference planes.

possible to obtain the ear prosthesis by directly casting the prosthetic material into the RP fabricated model (Task 5, Task 6). However, in this case study, neither the physical copy nor the prosthesis was constructed, since this experiment was a preliminary feasibility study to assess the generality of the method and to understand the performances of the instrument in the presence of undercuts and shadows.

4. Discussion and conclusions

Medical imaging systems (computerised tomography [CT] and magnetic resonance imaging [MRI]) in conjunction with RP machines have been proposed for the prosthetic restoration of facial defects (Watson *et al*. 1993, Chua *et al*. 1998a, Coward *et al*. 1999, Penkener *et al*. 1999, Webb 2000, Meinzer *et al.* 2002, Runte *et al.* 2002, Verdonk *et al.* 2003, Jiao *et al.* 2004). More recently, 3D whole-field profilometers based on the projection of incoherent light and 3D laser eye-safe scanners have been proposed as the acquisition devices, instead of CT and RMI systems. This trend is justified by (i) the complete lack of invasiveness for the patient, due to the pure-reflective approach to the measurement, (ii) the speed of the acquisition, which increases patient comfort and guarantees the accuracy of the measurements despite the unavoidable patient movements, (iii) the market availability of scanners at by far lower costs with respect to CT/MRI systems and (iv) their performance in terms of data quality, system portability and ruggedness.

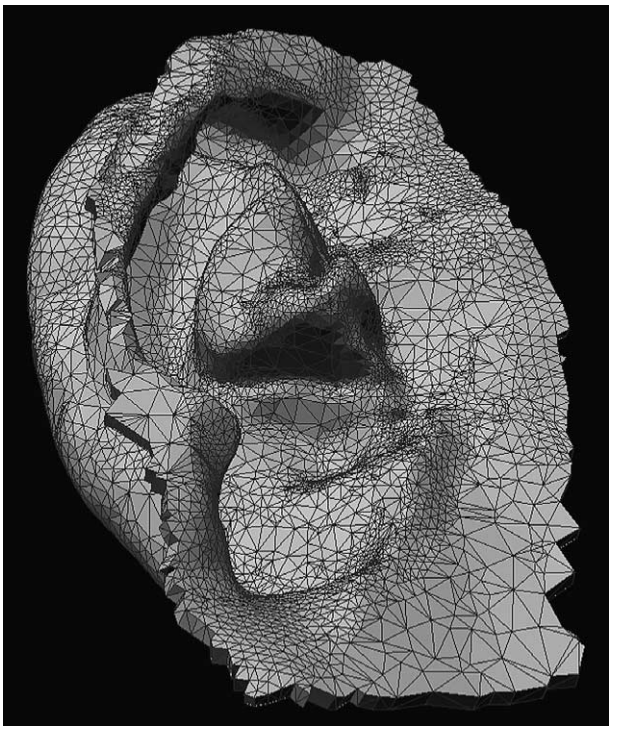

Figure 14. Modelling of the mould.

The combined use of optical acquisition, RE and RP techniques has been applied to the prosthetic restoration of ear loss (Cheah *et al.* 2003a, Leanne *et al.* 2004) and of eye defects (Reitemeier *et al.* 2004) and eye loss (Pan *et al.* 2007). The work is based on the use of non-coherent light devices. Suitable editing and mirroring of the raw 3D data result in CAD models that feed specialised RP machines, for the production of positive patterns. However, the process followed to obtain the actual prosthesis starting from the corresponding positive pattern is the conventional one. Laser scanners are also used for the ear reconstruction. The process starts from the optical acquisition of a cast of the safe ear (Ciocca and Scotti 2004, Al Mardini *et al.* 2005). Subsequent steps are completely automatic, since the actual prosthesis is directly fabricated from the mirrored CAD model of the ear. However, error contribution due to human modelling cannot be neglected, due to the initial use of the physical, hand-made cast. Alternatively, the CAD model of the positive pattern of the ear is used to obtain the CAD model of the negative mould (Cheah *et al.* 2003b): the physical mould is then RP machined.

Direct measurement of the ear has been proposed (Lin *et al.* 1998, Chua *et al.* 2000). Optical acquisition, CAD modelling, RP fabrication and vacuum casting are combined to produce the prosthetic model. The method allows both the fabrication of the silicon mould and the direct RP fabrication of the mould. The experimental results highlight that the former route yields better performance of the final prosthesis. Further works propose the production of face physical models for surgery assessment and of breast replicas in cancer surgical ablation (Chua *et al.* 1998b) and laser acquisition of face defects and mould CNC fabrication (Tsuji *et al.* 2004).

The manufacturing system proposed in this work does not require initial casts, and, in principle, it uses RP to fabricate the physical mould, avoiding positive pattern fabrication. Hence, the dependence on the anaplasthologist skill is significantly reduced, and the overall process efficiency is increased. Patient comfort is optimal, since the acquisition step is quick, contactless and safe. The prosthesis try-in is not necessary and the patient can be involved in the virtual sculpturing of the prosthesis (i.e. the choice of the template shape and its refinement). This aspect is of primary importance, especially in view of the subsequent replacements of the prostheses, which are necessary due to colour changes, aging, contamination and loss of fit.

Accuracy of the reconstruction is guaranteed both by the measurement performance of the instrument and by its flexibility. Indeed, the digitiser can be reconfigured at the required resolution without any re-calibration. This characteristic is particularly relevant in view of guaranteeing the completeness of the acquisition, since it strongly reduces the editing time and allows the creation of the polygon mesh. The overall quality of the mesh makes it suitable for direct RP fabrication, avoiding further CAD editing.

Production of the physical mould is not expensive (in our case it cost 2000 euros). It is worth noting that the worst case has been presented here, because the whole face was prototyped. However, the extension of the reference and of the sculptured models can be reduced, depending on the defect.

The method is general: it inherently adapts to the restoration of any other facial defect, with or without symmetrical shapes. For example, it can be fruitfully used whenever the defect involves irregular regions around a single facial organ (e.g. the nose and part of one cheek, the forehead, the orbital and mastoid bone tissues).

References

Al Mardini, M., Ercoli, C. and Graser, G.N., 2005. A technique to produce a mirror-image wax pattern of an ear using rapid prototyping technology. *Journal of Prosthetic Dentistry*, **94**, 195–198.

Bernardini, F. and Rushmeier, H., 2002. The 3D model acquisition pipeline. *Computer Graphics Forum*, **21**, 149–172.

Beumer, G. III, Curtis, T.A. and Marunick, M.T., 1996. *Maxillofacial rehabilitation-prosthodontic and surgical considerations.* St. Louis: Ishiyaku Euro America.

Blais, F., 2004. A review of 20 years of range sensors development. *Journal of Electronic Imaging*, **13** (1), 231–240.

Brasier, S., 1954. *Maxillo-facial laboratory techniques and facial prostheses.* London: Henry Kimpton.

Cheah, C.M., *et al.*, 2003a. Integration of laser surface digitizing with CAD/CAM techniques for developing facial prostheses. Part 1: Design and fabrication of prosthesis replicas. *International Journal of Prosthodontology*, **16** (4), 435–441.

Cheah, C.M., Chua, C.K. and Tan, K.H., 2003b. Integration of laser surface digitizing with CAD/CAM techniques for developing facial prostheses. Part 2: Development of Molding Techniques for Casting Prosthetic Parts. *International Journal of Prosthodontology*, **16** (5), 543–548.

Cheah, C.M., *et al.*, 2005. Rapid prototyping and tooling techniques: a review of applications for rapid investment casting. *International Journal of Advanced Manufacturing Technology*, **25**, 308–320.

Chen, Y. and Medioni, G., 1992. Object modelling by registration of multiple range images. *Image Vision and Computing*, **10**, 145–55.

Chua, C.K., *et al.*, 1998a. An integrated experimental approach to link laser digitizer, CAD/CAM system and rapid prototyping system for biomedical applications. *International Journal of Advanced Manufacturing Technology*, **14**, 110–115.

Chua, C.K., *et al.*, 1998b. Rapid prototyping assisted surgery planning. *International Journal of Advanced Manufacturing Technology*, **14** (9), 624–630.

Chua, C.K., *et al.*, 2000. Facial prosthetic model fabrication using rapid prototyping tools. *Journal of Manufacturing Technology Management*, **11** (1), 42–53.

Ciocca, L. and Scotti, R., 2004. CAD-CAM generated ear cast by means of a laser scanner and rapid prototyping machine. *Journal of Prosthetic Dentistry*, **92**, 591–595.

Coward, JJ., Watson, R.M., and Wilkinson, I.C., 1999. Fabrication of a wax ear by rapid process modeling using stereolithography. *International Journal of Prosthodontology*, **12**, 20–7.

Guidi, G., *et al*., 2003. 3D acquisition of Donatello's Maddalena: protocols, good practices and benchmarking. *Proceedings Electronic Imaging & the Visual Arts: EVA,* 174–178.

Jiao, T., *et al.*, 2004. Design and fabrication of auricular prostheses by CAD/CAM system. *International Journal of Prosthodontology*, **17** (4), 460–463.

Konica Minolta Sensing, Inc., 2002. *Vivid 910 Non-Contact 3D digitizer* [online]. Available from: www.minolta3d.com [accessed 10 March 2009].

Leanne, M., *et al.*, 2004. Applications of rapid prototyping technology in maxillofacial prosthetics. *International Journal of Prosthodontology*, **17** (4), 454–459.

Lemon, J.C., *et al.*, 1996. Technique for fabricating a mirror-image prosthetic ear. *Journal of Prosthetic Dentistry*, **75**, 292–293.

Lin, S.C., Chua, C.K., and Chou, S.M., 1998. A novel technique for fabricating facial prosthetic models. *The 20th Annual International Conference of the IEEE Engineering in Medicine and Biology Society (EMBS'98)*, Hong Kong.

Meinzer, H.P., *et al.*, 2002. Medical imaging: examples of clinical applications. *ISPRS J. Photogramm. Rem. Sen*, **56**, 311–325.

Pan, J., Zhao, Y. and Su, F., 2007. Application of phase measuring profilometry in reconstructing a 3D digitizing face model with open eyes. *Journal of US-China Medical Science*, **4** (1), 51–54.

Penkener, K., *et al.*, 1999. Fabricating auricular prostheses using three-dimensional soft tissue models. *Journal of Prosthetic Dentistry*, **82**, 482–4.

Reitemeier, B., *et al.*, 2004. Optical modelling of extraoral defects. *Journal of Prosthetic Dentistry*, **91**, 80–84.

Roberts, A.C., 1971. *Facial prostheses.* London: Henry Kimpton.

Runte, C., *et al.*, 2002. Optical data acquisition for computer-assisted design of facial prostheses. *International Journal of Prosthodontology*, **15**, 129–132.

Sansoni, G., Trebeschi, M. and Docchio, F., 2009. State-of-the-art and applications of 3D imaging sensors in industry, cultural heritage, medicine, and criminal investigation. *Sensors*, **9** (1), 568–601.

Taylor, T.D., 2000. Clinical maxillofacial prosthetics. *Quintessence*, 245–64.

Tsuji, M., *et al.*, 2004. Fabrication of a maxillofacial prosthesis using a computer-aided design and manufacturing system. *Journal of Prosthodontology*, **13**, 179–83.

Verdonk, H.W.D., *et al.*, 2003. Computer-assisted maxillofacial prosthodontics: a new treatment protocol. *International Journal of Prosthodontology*, **16**, 326–328.

Watson, R.M., *et al.*, 1993. Considerations in treatment planning for implant-supported auricular prostheses. *International Journal of Oral Maxillofacial Implants*, **8**, 688–94.

Webb, P.A., 2000. A review of rapid prototyping (RP) techniques in the medical and biomedical sector. *Journal of Medical Engineering Technology*, **24**, 149–153.